Chemisorption of manganese phthalocyanine on Cu(001) surface promoted by van der Waals interactions

S. Javaid,[1] S. Lebègue,[2] B. Detlefs,[3,*] F. Ibrahim,[1] F. Djeghloul,[1] M. Bowen,[1] S. Boukari,[1] T. Miyamachi,[4] J. Arabski,[1] D. Spor,[1] J. Zegenhagen,[3] W. Wulfhekel,[4] W. Weber,[1] E. Beaurepaire,[1] and M. Alouani[1]

[1]*Institut de Physique et de Chimie des Matériaux de Strasbourg and NIE UMR 7504, Université de Strasbourg-CNRS, 23 rue du Loess, Boîte Postale 43, 67034 Strasbourg Cedex 2, France*

[2]*Laboratoire de Cristallographie, Résonance Magnétique et Modélisations (CRM2, UMR CNRS 7036), Institut Jean Barriol, Nancy Université Boîte Postale 239, Boulevard des Aiguillettes 54506 Vandoeuvre-lès-Nancy, France*

[3]*European Synchrotron Radiation Facility (ESRF) Boîte Postale 220, 38043 Grenoble, France*

[4]*Physikalisches Institut and Center for Functional Nanostructures, Karlsruhe Institute of Technology, Wolfgang-Gaede-Strasse 1, 76131 Karlsruhe, Germany*

(Received 8 June 2012; revised manuscript received 15 March 2013; published 17 April 2013)

van der Waals (vdW) interactions within density functional theory are shown to strongly reduce the distance between manganese phthalocyanine (MnPc) and a Cu(001) surface to that found by x-ray standing wave experiments. Thus, the physisorbed ground state that is predicted within the generalized-gradient approximation formalism is replaced by a chemisorbed ground state once vdW interactions are taken into account. These findings indicate how to systematically obtain the correct theoretical adsorption distance for complex molecules and thus accurately predict the properties of the ensuing molecule/metal interface. The reduction of the experimental work function upon molecular adsorption is satisfactorily accounted for and explained in terms of Friedel-like oscillations of the charge density at the vicinity of the MnPc molecule that change the sign of the charge transfer electric dipole. This shows how vdW interactions can strongly impact charge injection in organic electronic devices.

DOI: 10.1103/PhysRevB.87.155418 PACS number(s): 68.43.−h, 71.15.Nc, 71.20.−b

I. INTRODUCTION

Simple yet powerful concepts describe how charges may flow from a device's metallic electrode into the active organic layer of an electronic device. The M/OS interface between a metal (M) and an organic semiconductor (OS) may exhibit a charge dipole that reflects the poor screening of the metal's charge into the OS away from the interface. The ensuing change to the metal's work function can in turn strongly affect the flow of charge, and as such should be taken into consideration at the device design stage.

More careful studies of the interface between a metal and the molecules that form the OS have helped refine these basic concepts, but have especially drawn attention to the very rich properties that the M/OS interface may possess.[1,2] For example, the mechanism of molecular adsorption onto the metal surface may play a crucial role in promoting metallic properties on the interfacial molecules,[3] with interesting repercussions within the emerging field of organic spintronics.[4–10]

In order to predictably design organic electronics components that can wield these promising interfacial properties, several model systems are being studied[11–16] to understand the subtle balance between OS-OS and M-OS interactions. Combining metal phthalocyanines and other planar molecules with various noble metal surfaces[16–21] allows tuning of the bonding strength between the OS and the substrate. The molecular properties can easily be changed by substituting the central metal atom and the observed structures often change with coverage[22] and temperature.[23]

For an accurate description of the adsorption geometry a combination of several experimental techniques is used. The lateral adsorbate structure is usually studied by scanning tunneling microscopy (STM)[24,25] and low-energy electron diffraction.[20–22] The local probe techniques rely on an electronic (STM) or a force-field (atomic force microscopy) interaction between a tip and the object of interest, and thus offer at best an indirect determination of the molecule-to-surface distance. The vertical distances can be determined by an x-ray standing wave experiment (XSW).[11,26] These experiments allow one to also study distortions of the planar OS upon adsorption.[11,22,27–30] For example, while the previous XSW study of naphthalene tetracarboxylic anhydride on Ag(111) did not mention any distortion of the molecule,[18] a relatively recent study found that the the carboxylic oxygen atoms at the corners of the molecule are located about 1/4 Å closer to the topmost Ag atoms than the naphthalene core.[29]

Conversely, theoretical frameworks to model both metals and OSs are only presently beginning to converge so as to account for not only ionic and covalent bonds, but also weak van der Waals (vdW) interactions that equally influence the molecule-to-surface distance.[31–35]

We have studied manganese phthalocyanine molecules deposited on a Cu(001) surface. With several chemical species and bonding environments involved, simple models are often insufficient to describe the rich physics present. In particular, we will show that different theoretical treatments can lead to fundamentally contrasting descriptions of the adsorption mechanism and of the resulting electronic properties of the metal/molecule interface. Only when vdW interactions are correctly taken into account can the experimentally observed physics be accurately computed. We focus on the technologically important evaluation of work function change due to molecular adsorption. Our work describes an overall general theoretical methodology that can be applied to accurately describe any molecule/surface system by correctly pinpointing the molecular adsorption distance.

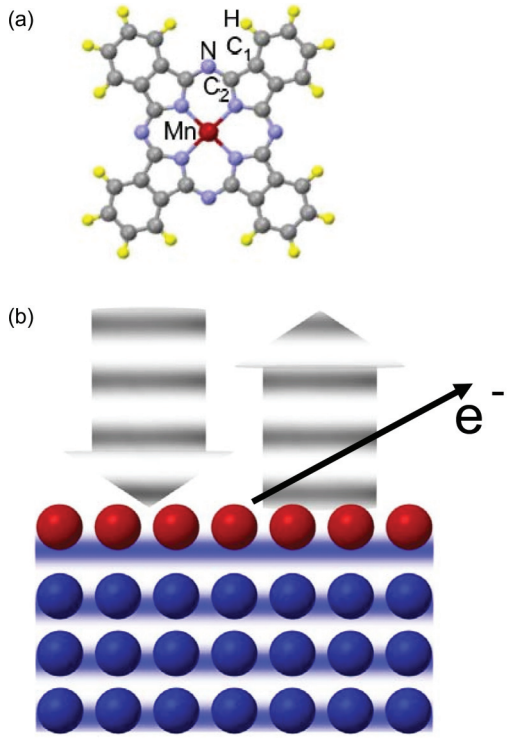

FIG. 1. (Color online) Phthalocyanine molecule on Cu(001). (a) The manganese phthalocyanine molecule contains a Mn ion bridged by four N ligands of a pyrrole ring that is extended by a benzene ring. (b) Schematic of XSW experiment. An x-ray beam close to normal incidence diffracts off of the Cu lattice (blue) and places the atomic sites (red) of the adsorbed molecule within an x-ray standing wave field.

By virtue of their planar geometry and numerous atomic species with varying chemical environment [see Fig. 1(a)], phthalocyanine (Pc) molecules represent an ideal candidate to elucidate how to reconcile theory with experiment. Indeed, Pc molecules generally adsorb in a qualitatively flat manner on surfaces,[3,5,32] including the prototypical Cu(001) surface.[6]

II. METHOD OF CALCULATION

Density functional theory (DFT) calculations were carried out by means of the ultrasoft pseudopotential method[36] as implemented in the PWSCF package.[37] For the exchange-correlation potential, we used the generalized gradient approximation (GGA) as parametrized by Perdew, Burke, and Ernzerhof.[38] A kinetic energy cutoff of 30 Ry has been used for the plane-wave basis set. For the convergence of the charge density, we used a cutoff of 300 Ry. Because the aim is to study a single molecule on metallic surfaces, we used only the gamma point to sample the first Brillouin zone. The surface of Cu(001) has been modeled by using periodic supercells of three atomic layers of (8×8) atoms separated by a vacuum region. The lattice vector perpendicular to the surface is 30 nm. It has been shown that three monolayers of Cu are sufficient to obtain well-converged results.[33] We have, in particular, confirmed that the work function of copper does not change much if five rather than three copper layers are used.[33] vdW interactions were computed within the GGA-D2 approach developed by Grimme[39] and later implemented in the PWSCF package by Barone and co-workers.[40] These calculations were also conducted with the Vienna *ab initio* simulation package (VASP)[41,42] using the projector augmented wave basis set[43] and Grimme's scheme for the vdW interactions.[44] We used exactly the same input parameters as for the PWSCF calculation and obtained the same results. To understand the unexpected change of the metal work function upon molecular adsorption, Löwdin population analysis was used to determine the net charge on the adsorbed MnPc molecule.[45] We find a net electron Löwdin transfer from Cu(001) to MnPc of 0.24 electrons in the GGA-unrelaxed case and 2.60 electrons for the GGA-relaxed case including vdW interactions. Our calculations based on VASP and Bader analysis[46] also confirm the charge transfer both within GGA and GGA + U which show a charge transfer towards the molecule of about 1.34 and 1.32 electrons, respectively. The latter charge transfer is much smaller than the one obtained using the PWSF and Löwdin analysis but are qualitatively in agreement. Thus, within a charge transfer picture, one would expect the work function of MnPc on Cu(001) to increase relative to that of Cu(001). Including improved electronic correlations on the Mn site using GGA + U with $U = 4$ eV and $J = 1$ eV does not significantly change either the adsorption distance or the charge transfer. However, the density of states are strongly modified on the Mn site.

III. X-RAY STANDING WAVE MEASUREMENTS

To experimentally measure the distance between the atomic sites of manganese Pc and Cu(001) with a high degree of precision, we used the XSW technique[26] on beamline ID32 at the European Synchrotron Radiation Facility (ESRF) in Grenoble, France. The x-ray beam was shaped to 0.6 mm × 0.4 mm, monochromatized by a double Si(111) crystal ($\Delta E/E = 1.3 \times 10^{-4}$). The planar XSW is formed thanks to (002) Bragg diffraction from the Cu single-crystal substrate [refer to Fig. 1(b)] and is therefore periodic with the (002) planes. All XSW experiments were performed at near-normal incidence with respect to the scatterer planes [Cu(002), 3.432 keV], and at room temperature. Every molecular site will absorb x-ray photons and then emit photoelectrons proportionately to the local intensity of this periodic x-ray field. By scanning the photon energy so as to pass the Bragg condition, the phase between the incident and reflected beams shifts by π and the position of the XSW is shifted by half the (002) lattice spacing $d_{(002)}$, which alters the intensity of the electric field on a given atomic site. By recording the photoelectron yield in the standing wave, we can retrieve the position of chemically distinct species relative to that of the Cu planes. Photoelectron yield curves were derived from the integrated Mn-2$p_{3/2}$, C-1s, N-1s, and Cu-2$p_{3/2}$ signals after subtracting the Shirley background. After an initial larger Mn-2p region scan to exclude overlap with another XPS/Auger line, only the Mn-2$p_{3/2}$ peak of the XPS signal was recorded so as to improve the signal-to-noise ratio of this low-intensity signal. The very strong inelastic background[47] on the high binding energy side of the Mn-2p states may be explained by the fact that Mn atoms are positioned below the average height of the MnPc molecule as shown by our experiment. The overall

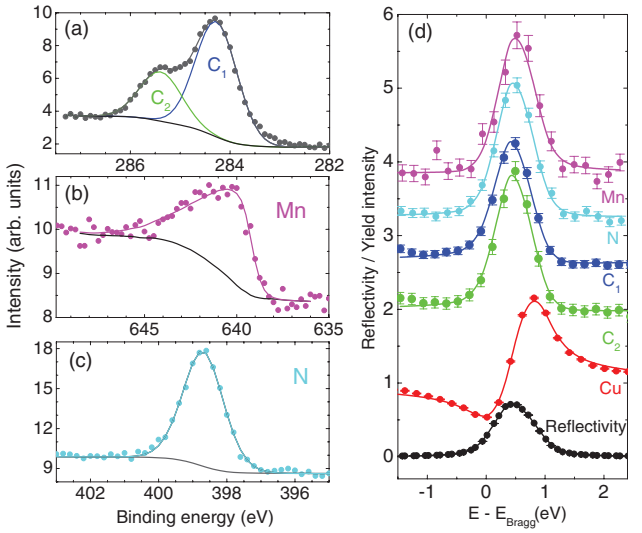

FIG. 2. (Color online) X-ray standing wave measurements of MnPc on Cu(001). The core-level photoelectron spectra recorded for a photon energy near the Bragg condition for (a) C 1s, (b) Mn 2$p_{3/2}$, and (c) N 1s are fitted, using two components for C, to obtain the photoelectron yield. (d) This photoelectron yield is then measured while tuning the incoming photon energy across the Bragg condition [$E_{\mathrm{Bragg}} = 3.432$ keV, $Q = (002)$]. Fitting of the ensuing data yields the site-specific adsorption distance from the Cu(002) scattering planes. Datasets were shifted for clarity.

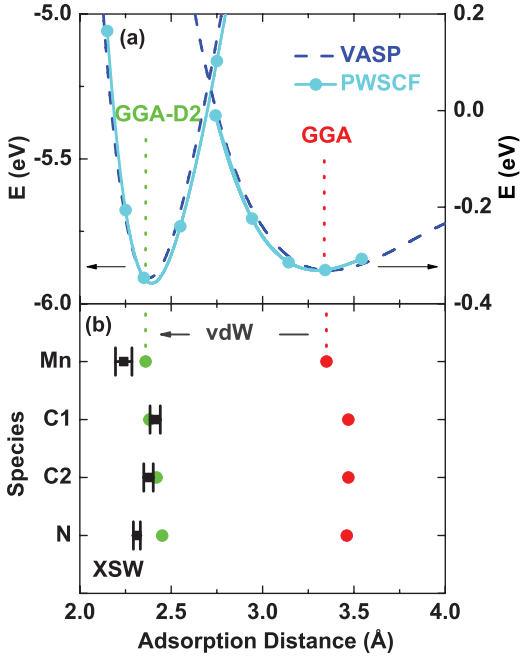

FIG. 3. (Color online) (a) Calculated adsorption energy E in eV of MnPc on Cu(001) surface within PWSCF (solid curves with dots) and VASP (dashed curves), and (b) comparison between measured and calculated distances between the Cu(001) surface and various MnPc atoms. The adsorption energy (top panel) as a function of the distance of Mn from Cu(001) reveals that GGA-D2 calculations peg the Mn-to-Cu distance in good agreement with XSW experiments. The adsorption energy with and without vdW interaction is -5.9 eV and -0.32 eV per MnPc molecule, respectively. The experimental (black squares) and theoretical (dots) distances between the atomic species of the MnPc molecule and the Cu(001) surface are in good agreement with GGA-D2 (green) results.

energy resolution used in the XSW measurements was not sufficient to distinguish between N-C and N-Mn bonds in the N-1s XPS spectra that had be fitted with a single peak function. Various peak integration methods (various asymmetric peak profiles, numerical integration, various background choices) were tested in order to estimate the systematic error originating from the particular choice.

MnPc molecules were deposited ($P = 2 \times 10^{-9}$ mbar) onto atomically clean and flat Cu(001) surfaces to a coverage of 1 monolayer (ML). X-ray photoelectron spectroscopy (XPS) was used to rule out any surface contamination. We present in Fig. 2 typical C-1s [panel (a)], Mn-2$p_{3/2}$ [panel (b)], and N-1s core-level photoemission spectra recorded at $T = 300$ K for a photon energy near the Bragg condition. Two different approaches to the analysis of the C-1s photoemission spectra were employed: In the first one, two distinct peaks, identified in Fig. 2(a) as C_1 and C_2, were attributed to carbon sites in the benzene and pyrrole environments. Relaxed energy resolution used in the XSW experiment did not allow us to separate the shake-up satellites from both carbon species[48,49] located about 1.9 eV above their main peaks.[50] This fact does not affect our interpretation of the XSW signal for benzene carbon but, because of an overlap between the main pyrrole peak and the shake-up satellite of the benzene peak, XSW parameters derived from the C_2 peak have to be taken with caution. The shake-up satellite contribution is difficult to estimate because the intensity ratio 3 : 1 between the benzene and pyrrole components expected in the off-Bragg condition has not been found before in MnPc.[51] In the second approach the assignment to individual chemical species components is not considered and only the overall integrated intensity for the C-1s spectra is determined. In neither of the analysis approaches has the broad high-binding energy side satellite structure of the C1s spectra been included due to the limited binding energy range chosen during the experiment.

By fitting the XPS peaks one may extract the integrated intensity which corresponds to the photoelectron yield for a given photon energy. We then vary the photon energy across the Bragg condition and track the photoemission response.[26] Representative XSW data are shown in Fig. 2(c) for all relevant atomic species. Fitting these data reveals the coherent position P_{eff}, which is the average distance from the Cu(002) plane, and the coherent fraction F_{eff}, which is a measure of the distribution of these positions. Table I and Fig. 3 summarize both the experimentally obtained results and the simulated coherent fractions and coherent positions. Our XSW results show that, due to adsorption, the molecule is no longer planar. While the Mn site is lowered toward the substrate, the N and C sites tend to lie further away at 2.4 Å from the Cu(001) surface.

IV. RESULTS AND DISCUSSION

A. Stability of the MnPc molecule on Cu(001) substrate

In a previous work, we used a GGA framework to predict that MnPc lies 3.6 Å away from a Cu(001) surface.[6] But, the

TABLE I. Experimental and GGA and GGA-D2 calculated atomic positions of MnPc on Cu(001). Here F_{eff} is the coherent fractions and P_{eff} the coherent positions. The last line corresponds to the analysis of the average carbon position.

	XSW experiment			GGA	
Species	F_{eff}	P_{eff}	d (Å)	d (Å)	GGA-D2
Cu	0.90 ± 0.05	0.010 ± 0.005	3.631 ± 0.009		
Mn	0.80 ± 0.08	0.240 ± 0.025	2.240 ± 0.045	3.35	2.36
N	0.78 ± 0.10	0.280 ± 0.010	2.312 ± 0.019	3.46	2.45
C_1	0.60 ± 0.10	0.335 ± 0.015	2.412 ± 0.028	3.46	2.38
C_2	0.68 ± 0.10	0.315 ± 0.015	2.376 ± 0.026	3.46	2.42
C	0.58 ± 0.10	0.333 ± 0.015	2.403 ± 0.028	3.46	2.39

XSW experiments reveal a surprisingly much closer distance between the atomic sites of MnPc and the Cu(001) surface. We unravel the apparent contradiction by examining more closely how DFT needs to be refined by including vdW weak interactions so as to accurately reproduce the experimentally observed distance.

Figure 4(a) shows the top view of MnPc adsorbing in the bridge position onto Cu(001). The molecule experiences very little distortion within a relaxed GGA framework, as Mn is found to lie 0.11 Å closer to the Cu surface than the other molecular sites. The small change in adsorption distance from 3.6 to 3.35 Å due to relaxing the structure does not lead to significant interfacial bonding [see Fig. 4(c)]. As a result, the Mn partial density of states (PDOS) of MnPc on Cu(001) essentially resembles that of a free molecule, so that little charge density is shared between the molecular sites and the Cu surface [Fig. 4(c)]. Thus, according to standard GGA, MnPc is essentially physisorbed[52] onto Cu(001).

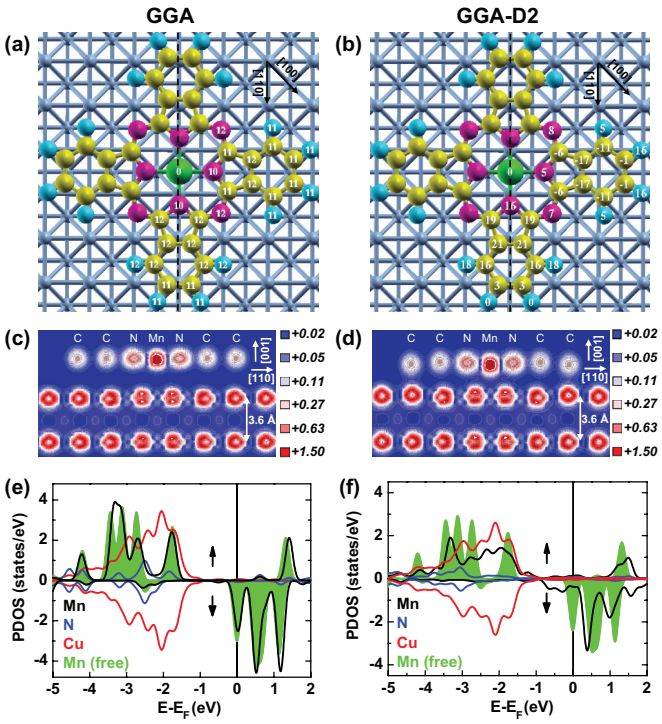

FIG. 4. (Color online) Calculated adsorption geometry and electronic structure of MnPc on Cu(001). (a) GGA calculations show that the otherwise planar MnPc molecule exhibits little distortion upon relaxing the structure. However, including vdW dispersive forces leads to molecular distortion (b), such that one benzopyrrole group points upwards, while the neighboring one points downwards. The number in each atomic sphere represents the deviation (numbers given in 10^{-2} Å) from the plane of Mn parallel to the substrate. Panels (c) and (d) show the charge density along the dashed line of panels (a) and (b) within the (110) plane. Panels (e) and (f) respectively show the PDOS without and with vdW forces. Including vdW forces alters the adsorption distance and the adsorption mechanism of MnPc on Cu(001). Due to the resulting hybridization, the Mn PDOS no longer resembles that found for a free molecule.

We can theoretically reproduce the experimentally determined molecular adsorption distance *in a reasonably good quantitative manner* by including vdW weak interactions.[53] As seen in Fig. 3(a), the adsorption energy of MnPc on Cu(001), given by the difference of the total energy of the whole system minus those of the substrate and of the free MnPc molecule, is minimized for a Mn-Cu distance that is ≈1 Å smaller upon including vdW dispersive forces. Referring to Fig. 3(b) and Table I, we now find a relatively good quantitative agreement between theory and experiment on the Mn-Cu and N-Cu distances (the maximum deviation from experiment is less than 0.14 Å and is for the average position of the N atoms). The agreement with experiment becomes excellent regarding the positions of the C atoms. This quantitative agreement between experiment and theory underscores the fact that the MnPc adsorption onto Cu(001) causes the molecule to lose its planar symmetry. Indeed, referring to Fig. 4(b), one benzopyrrole group now points upwards, while the neighboring one points downwards. The adsorption energy changes from the GGA value of −0.32 eV per MnPc molecule to −5.9 eV upon adding vdW interactions. This important change is reasonable owing to the large size of the MnPc molecule. These results are similar to the theoretical results of Cuadrado *et al.*[54] regarding CoPc on Cu(111). They also found that vdW interactions lower the symmetry of the molecule from C4 to C2 in agreement with STM images. The adsorption of CuPc on Cu(111) was also shown by STM to have a reduced symmetry, i.e., the two opposite lobes of the molecule appear higher than adjacent lobes. This change of the fourfold to a twofold symmetry was attributed to the adsorption geometry.[55] More complex distortions were also found for cobalt and iron porphyrins when adsorbed on Ag(111),[56] whereas calculation without vdW interaction of a 1,4,5,8-naphthalene-tetracarboxylic-dianhydride molecule on the Ag(110) surface did not show any distortion.[57]

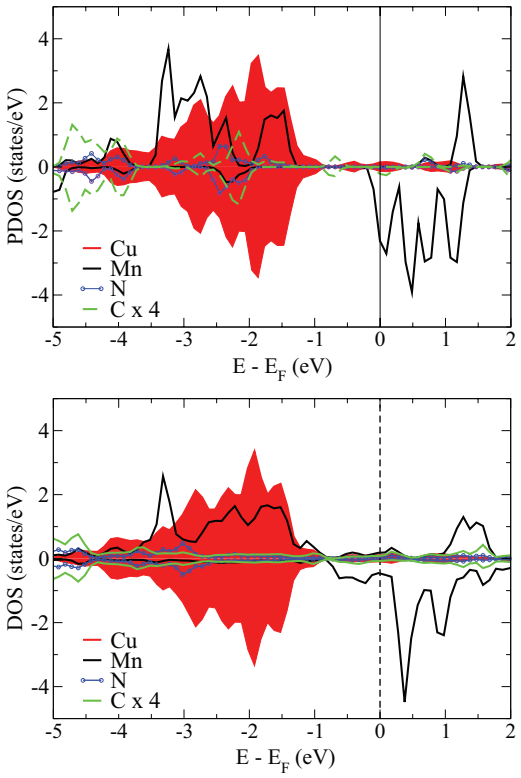

FIG. 5. (Color online) GGA + vdW-calculated PDOS of the MnPc molecule far from (5.5 Å, top panel) and close to (2.2 Å, lower panel) the Cu(001) surface. The HOMO and LUMO of the molecule are transformed into hybrid molecular orbitals due to the strong interaction with the Cu(001) surface.

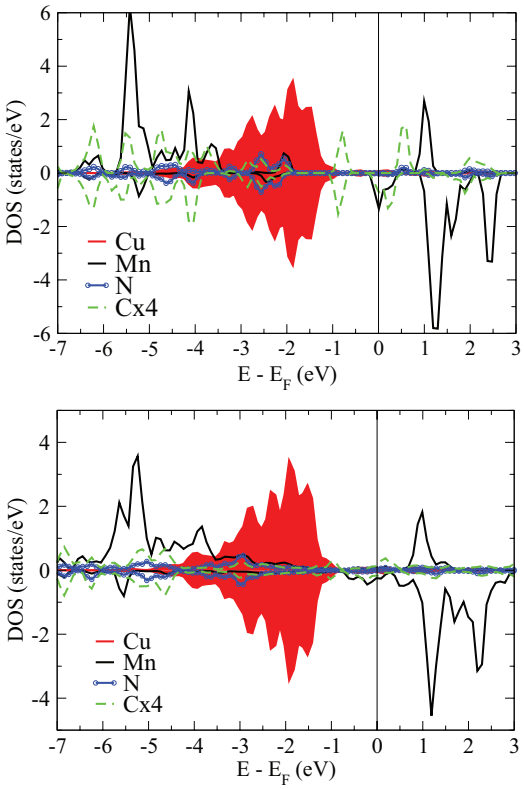

FIG. 6. (Color online) GGA + U + vdW-calculated PDOS of the MnPc molecule far from (5.5 Å, top panel) and close to (2.2 Å, lower panel) the Cu(001) surface. Here $U = 4$ eV and $J = 1$ eV. The HOMO and LUMO of the molecule are transformed into hybrid molecular orbitals due to the strong interaction with the Cu(001) surface.

B. Electronic and magnetic properties of MnPc molecule on Cu(001) substrate

Since we have determined how DFT + vdW can accurately reproduce the experimental molecular adsorption distance, how does DFT + vdW *now* describe the resulting system? GGA, whether unrelaxed or relaxed, reveals little change to the molecular orbitals of MnPc upon molecular adsorption onto Cu(001). This picture of physisorption[52] may be naively expected since Cu is a noble metal.[3,6] Yet, as seen in Fig. 4(d) and due in large part to the closer molecular adsorption distance, including atomic relaxation and vdW dispersive forces thanks to GGA-D2 theory describes a picture of interfacial hybridization as revealed by charge contours propagating from the Cu(001) surface to the molecular sites promoting chemisorption. As a result, the Mn PDOS shares features of the Cu PDOS, and in particular has more states below the Fermi level in the spin ↓ channel, which is generally broadened [see Fig. 4(f)]. This increase in spin ↓ population leads to a reduction in the Mn calculated magnetic moment from 3.47μ_B for the free MnPc to 3.05μ_B once vdW interactions are taken into account. Similar calculations for MnPc on Co(001), which is already chemisorbed within the GGA framework, show that including vdW interactions has only a little effect on the molecule's adsorption distance and thus on its electronic structure.[58]

Here we provide some further information concerning the adsorption of the MnPc molecule on the Cu(001) surface. The spin-polarized PDOS per atom is plotted in Fig. 5 for two distances between the molecule and the substrate. It can be seen from Fig. 5 that, when the molecule is far from the surface at about 5.5 Å, we can distinguish both the highest occupied molecular orbital (HOMO) and the lowest unoccupied molecular orbital (LUMO) of the free molecule. When the MnPc molecule interacts strongly with the substrate at the equilibrium distance of 2.36 Å, then the PDOS of each atom of the molecule is transformed by the interaction with the Cu(001) surface. Figure 5(b) shows that the PDOS become more extended by hybridizing with the Cu(001) states. As a result the band gap between the LUMO and HOMO is completely smeared out.

The magnetism of the MnPc molecule is driven by Mn 3d orbitals. In order to describe the effect of the metallic substrate on magnetic properties of MnPc, we have compared in Figs. 5 and 6 the PDOS of Mn of MnPc deposited on Cu(001) and with that of Mn 3d of MnPc molecule away from the surface, calculated respectively within the GGA + vdW and GGA + U + vdW. We observe that Mn PDOS for free molecule and MnPc/Cu are different, showing that MnPc on Cu has a magnetic state which is not the same as that of the free molecule. In particular, we observe that the majority Mn spin PDOS is considerably broadened due to the interaction of the molecule with the substrate, and the minority PDOS is also broadened below the Fermi level. The calculated magnetic

TABLE II. PWSCF and VASP (within parentheses) calculated GGA + vdW magnetic moments of Mn in MnPc at 5.5 Å and 2.36 Å from the Cu(001) surface. The induced total magnetic moment on all N and C are also given. The VASP values are also given for comparison.

	GGA + vdW		GGA + U + vdW	
Distance	5.5 Å	2.36 Å	5.5 Å	2.36 Å
Mn	$3.47\mu_B$ (3.17)	$3.05\mu_B$ (2.77)	(3.46)	(3.34)
N	$-0.15\mu_B$ (-0.13)	$-0.11\mu_B$ (-0.10)	(-0.14)	(-0.13)
C	$-0.08\mu_B$ (-0.07)	$-0.26\mu_B$ (-0.3)	(-0.15)	(-0.27)

moment of Mn is given in Table II together with the induced magnetic moment on nitrogen and carbon atoms. When the molecule is far away from the surface, the induced magnetic moment for the carbon atoms which is of $-0.0025\mu_B$/atom ($-0.005\mu_B$/atom in GGA + U) is negligible, while that of nitrogen is $-0.019\mu_B$/atom. The minus sign is due to the hybridization of a less-than-half-filled orbital with a more-than-half-filled one. When the molecule is closer to the surface, the Mn magnetic moment is strongly reduced to $3.05\mu_B$/atom. The reduction is due to the charge transfer from the Cu(001) towards the molecule. It is interesting to notice that the charge transfer somewhat reduces the overall magnetic moment of the nitrogen atoms but increases by about a factor of 3 that of the carbon atoms. The reduction of the Mn magnetic moment in GGA + U is much smaller due to the localization of the Mn $3d$ states due to the Coulomb interaction.

C. Change of Cu(001) work function due to MnPc adsorbate

This interface hybridization in turn alters the potential profile at the metal/molecule interface. Prior to molecular adsorption, the energy positions of the molecule's orbitals and of the metal's Fermi level are defined with respect to the vacuum potential. Upon adsorption, these levels are thought to shift rigidly due, in part, to the formation of an interface dipole that reflects the poor charge screening from the molecule. Generally, one assumes that, if there is a net transfer of electrons from a metal to the adsorbed molecule, then the effective work function shall increase relative to that of the bare metal.[2] Yet, interestingly, this is only sometimes the case. For example, despite a net transfer of charge onto Pc molecules that should lead to a work function increase, using an electron scattering experiment by monitoring the secondary electron energy cutoff, we find that the work function of Cu(001), at room temperature, decreases by 0.74 eV for 1 ML MnPc on Cu(001). In what follows, we go beyond the standard dipole model and examine how the electronic charge is spatially distributed across the interface.

For MnPc on Cu(001), the change in work function $\Delta\Phi$ is $\Delta\Phi = \Phi_{\mathrm{MnPc/Cu}} - \Phi_{\mathrm{Cu}}$, where Φ_{Cu} and $\Phi_{\mathrm{MnPc/Cu}}$ are the work functions of Cu and MnPc adsorbed onto Cu, respectively. Calculations were done for 0.45 ML MnPc on Cu(001). In a naive picture of charge transfer from Cu(001) to MnPc, one should expect a positive $\Delta\Phi$. Yet *ab initio* GGA theory pegs $\Delta\Phi$ at -0.14 eV. This value, of opposite sign to what was naively expected, changes to -0.45 eV once vdW dispersive forces are accounted for and is now in good agreement

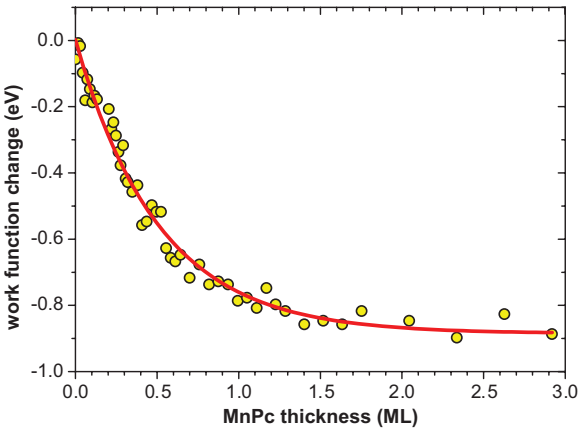

FIG. 7. (Color online) Experimental change of the work function of MnPc/Cu(001) for different MnPc coverage. The full line is a guide to the eye.

with the -0.52 ± 0.07 eV found experimentally for the same coverage. The change in work function upon covering Cu(001) with MnPc molecules was measured in an electron scattering experiment by monitoring the secondary electron energy cutoff. The results of this experience at room temperature are shown in Fig. 7. The absolute value of the reduction of the work function increases with increasing MnPc coverage and appears to saturate at about -0.9 eV above 1.5 monolayer.

To resolve this apparent contradiction, we examine how charge is reorganizing across the interface due to molecular adsorption. We present in Fig. 8 the evolution $\Delta\rho(z)$ of the interface dipole that is spatially averaged along planes parallel to the Cu(001) surface: $\Delta\rho(z) = \rho_{\mathrm{MnPc/Cu\ slab}}(z) - \rho_{\mathrm{Cu\ slab}}(z) - \rho_{\mathrm{MnPc}}(z)$.

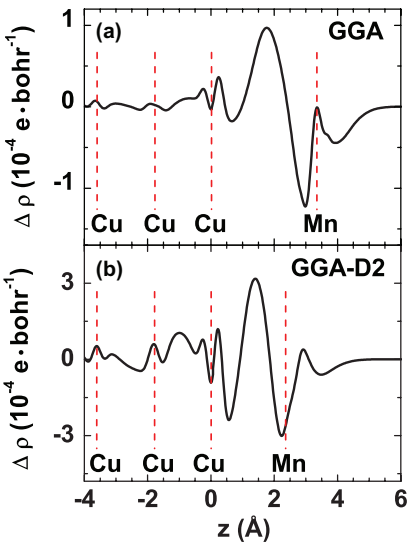

FIG. 8. (Color online) Calculated charge transfer due to molecular adsorption. The difference in planar charge density $\Delta\rho(z)$ between the MnPc and Cu(001) elements before and after adsorption is represented as a function of the distance away from the Cu(001)‖MnPc interface by integrating the charge density within planes normal to the interface. We consider the (a) GGA-unrelaxed and (b) relaxed GGA-D2 theoretical frameworks. Dashed lines indicate the position of the topmost Cu layer and of the molecule's Mn plane.

Rather than a rigid shift in molecular orbitals, the interface dipole in fact consists of Friedel-like oscillations that more realistically reflect how Cu is screening the interface charge due to molecular adsorption. However, closer to the molecular sites, a negative amplitude of $\Delta\rho(z)$ is also observed. We ascribe this oscillation to the chemical hybridization that is occurring between the molecule and the substrate. Comparing Figs. 8(a) and 8(b) shows how the reduction in the molecular adsorption distance due to vdW interactions leads to a nearly threefold increase in the amplitude of all oscillations in $\Delta\rho(z)$, including a substantial change in negative $\Delta\rho(z)$ near the molecular plane. Within a Friedel picture, this reflects the closer distance of the screened impurity to the Cu surface due to vdW interactions. Beyond the naive picture of charge transfer, this shows how treating the molecular adsorption onto a metal substrate—and in particular the adsorption distance—within the correct theoretical framework can yield the correct sign and amplitude of the ensuing change in the metal's work function.

As an alternate description of Fig. 8, we find that two well-known features lead to the adsorption-induced reduction in the work function. First, we observe an accumulation (positive peak) in the plot of the metallic electron density on the top surface layer of Co and a depletion (negative peak) in the electron density just above it. This is the well-known push-back or pillow effect,[59] which has been also studied for organic adsorbates.[60] The origin of the push-back effect is the Pauli repulsion, which results in the reduction of the work function consistently with our results. Secondly, a region of density depletion is present just above and below MnPc, accompanied by the accumulation of electron density at the interface. This effect can be attributed to the interfacial chemical bonding as the electrons that would be otherwise lying close to the MnPc plane are now engaged in hybridization at the center of the interface. This covalent bonding, present at the Co/MnPc substrate, is also known to reduce metallic work functions.[61,62] For MnPc/Cu, the planar averaged charge density calculated from GGA [Fig. 8(a)] reveals a much smaller charge reorganization (scales are ten times smaller) as compared to Co/MnPc. As a result, both chemical bonding and the push-back effect, even though present, are much weaker. For GGA-D2 [Fig. 8(b)], these effects become more pronounced due to the smaller adsorption distance and stronger interfacial interactions.

V. CONCLUSION

In conclusion, a careful comparison between theory and experiment has shown the importance of correctly modeling the molecular adsorption onto a metallic surface. Including van der Waals interactions without any parametrization within *ab initio* DFT yields adsorption distances for the numerous, chemically diverse sites of manganese phthalocyanine that are in reasonably good quantitative agreement with x-ray standing wave experiments. In turn, and independently of this experimental research track that is time consuming, and mostly limited to sublimable molecules, this enables DFT to correctly and *systematically* predict, for a given molecule/metal surface pair among many possible combinations, whether the molecule is physisorbed or chemisorbed. The research efficiency afforded by our results opens the possibility to accurately model the interfacial electronic properties induced by hybridization.[6,9] This will in turn help unravel how intrinsic molecular properties, such as a spin transition,[10,63] interact with these interfacial properties. Finally, it is now possible to systematically predict the adsorption-induced change in interface properties such as the work function so as to better engineer organic heterostructures for technological applications.

ACKNOWLEDGMENTS

We thank R. Mattana for experimental contributions, J. Duvernay for technical support, and J. Roy and F. Gautier for stimulating discussions. We acknowledge financial support from ANR PNANO Grants No. ANR-06-NANO-053-01 and No. ANR-06-NANO-053-02, the EC Sixth Framework Program (NMP3-CT-2006-033370), the CNRS-PICS Program No. 5275, the Deutsche Forschungsgemeinschaft (DFG), the Center for Functional Nanostructures (CFN) and the French German University, and the International Center for Frontier Research in Chemistry (FRC). S.J. thanks the Pakistani government (HEC) for financial support. This work was performed using HPC resources from GENCI-CINES Grant No. 2011-gem1100. We thank the Agence Nationale de la Recherche, project Labex NIE, for financial support.

*Present address: CEA-LETI, MINATEC Campus, 17 rue des Martyrs, 38054 Grenoble, France.

[1] J. C. Scott, J. Vac. Sci. Technol. A **21**, 521 (2003).
[2] Slawomir Braun, William R. Salaneck, and Mats Fahlman, Adv. Mater. **21**, 1450 (2009).
[3] A. F. Takács, F. Witt, S. Schmaus, T. Balashov, M. Bowen, E. Beaurepaire, and W. Wulfhekel, Phys. Rev. B **78**, 233404 (2008).
[4] H. Wende, M. Bernien, J. Luo, C. Sorg, N. Ponpandian, J. Kurde, J. Miguel, M. Piantek, X. Xu, Ph. Eckhold, W. Kuch, K. Baberschke, P. M. Panchmatia, B. Sanyal, P. M. Oppeneer, and O. Eriksson, Nature Mater. **6**, 516 (2007).
[5] C. Iacovita, M. V. Rastei, B. W. Heinrich, T. Brumme, J. Kortus, L. Limot, and J. P. Bucher, Phys. Rev. Lett. **101**, 116602 (2008).
[6] S. Javaid, M. Bowen, S. Boukari, L. Joly, J.-B. Beaufrand, Xi Chen, Y. J. Dappe, F. Scheurer, J.-P. Kappler, J. Arabski, W. Wulfhekel, M. Alouani, and E. Beaurepaire, Phys. Rev. Lett. **105**, 077201 (2010).
[7] C. Barraud, P. Seneor, R. Mattana, S. Fusil, K. Bouzehouane, C. Deranlot, P. Graziosi, L. Hueso, I. Bergenti, V. Dediu, F. Petroff, and A. Fert, Nat. Phys. **6**, 615 (2010).
[8] S. Sanvito, Nat. Phys. **6**, 562 (2010).
[9] S. Schmaus, A. Bagrets, Y. Nahas, T. K. Yamada, A. Bork, M. Bowen, E. Beaurepaire, F. Evers, and W. Wulfhekel, Nat. Nanotechnol. **6**, 185 (2011).
[10] T. Miyamachi, M. Gruber, V. Davesne, M. Bowen, S. Boukari, L. Joly, F. Scheurer, G. Rogez, T. Kazu Yamada, P. Ohresser, E. Beaurepaire, and Wulf Wulfhekel, Nat. Commun. **3**, 938 (2012).
[11] L. Kilian, W. Weigand, E. Umbach, A. Langner, M. Sokolowski, H. L. Meyerheim, H. Maltor, B. C. C. Cowie, T. Lee, and P. Bäuerle, Phys. Rev. B **66**, 075412 (2002).

[12]N. Koch, A. Gerlach, S. Duhm, H. Glowatzki, G. Heimel, A. Vollmer, Y. Sakamoto, T. Suzuki, J. Zegenhagen, J. P. Rabe, and F. Schreiber, J. Am. Chem. Soc. **130**, 7300 (2008).
[13]A. Hauschild, K. Karki, B. C. C. Cowie, M. Rohlfing, F. S. Tautz, and M. Sokolowski, Phys. Rev. Lett. **94**, 036106 (2005); **95**, 209602 (2005).
[14]G. Heimel, S. Duhm, I. Salzmann, A. Gerlach, A. Strozecka, J. Niederhausen, C. Bürker, T. Hosokai, I. Fernandez-Torrente, G. Schulze, S. Winkler, A. Wilke, R. Schlesinger, J. Frisch, B. Bröker, A. Vollmer, B. Detlefs, J. Pflaum, S. Kera, K. J. Franke, N. Ueno, J. I. Pascual, F. Schreiber, and N. Koch, Nat. Chem. **5**, 187 (2013).
[15]Y. Wang, J. Kröger, R. Berndt, and W. A. Hofer, J. Am. Chem. Soc. **131**, 3639 (2009); Y. Wang, K. Wu, J. Kröger, and R. Berndt, AIP Advances **2**, 041402 (2012).
[16]S. Duhm, S. Hosoumi, I. Salzmann, A. Gerlach, M. Oehzelt, B. Wedl, T.-L. Lee, F. Schreiber, N. Koch, N. Ueno, and S. Kera, Phys. Rev. B **81**, 045418 (2010).
[17]M. G. Roper, M. P. Skegg, C. J. Fisher, J. J. Lee, V. R. Dhanak, D. P. Woodruff, and R. G. Jones, Chem. Phys. Lett. **389**, 87 (2004).
[18]J. Stanzel, W. Weigand, L. Kilian, H. L. Meyerheim, C. Kumpf, and E. Umbach, Surf. Sci. Lett. **571**, L311 (2004).
[19]F. Allegretti, D. P. Woodruff, V. R. Dhanak, C. Mariani, F. Bussolotti, and S. D'Addato, Surf. Sci. **598**, 253 (2005).
[20]B. Stadtmüller, I. Kröger, F. Reinert, and C. Kumpf, Phys. Rev. B **83**, 085416 (2011).
[21]B. Stadtmüller, T. Sueyoshi, G. Kichin, I. Kröger, S. Soubatch, R. Temirov, F. S. Tautz, and C. Kumpf, Phys. Rev. Lett. **108**, 106103 (2012).
[22]I. Kröger, B. Stadtmüller, C. Stadler, J. Ziroff, M. Kochler, A. Stahl, F. Pollinger, T.-L. Lee, J. Zegenhagen, F. Reinert, and C. Kumpf, New J. Phys. **12**, 083038 (2010).
[23]C. Stadler, S. Hansen, I. Kröger, C. Kumpf, and E. Umbach, Nat. Phys. **5**, 153 (2009).
[24]M. Lackinger and M. Hietschold, Surf. Sci. **520**, L619 (2002).
[25]C. Bobisch, Th. Wagner, A. Bannani, and R. Möller, J. Chem. Phys. **119**, 9804 (2003).
[26]J. Zegenhagen, Surf. Sci. Rep. **18**, 199 (1993).
[27]A. Gerlach, F. Schreiber, S. Sellner, H. Dosch, I. A. Vartanyants, B. C. C. Cowie, T. L. Lee, and J. Zegenhagen, Phys. Rev. B **71**, 205425 (2005).
[28]C. Stadler, S. Hansen, F. Pollinger, C. Kumpf, E. Umbach, T.-L. Lee, and J. Zegenhagen, Phys. Rev. B **74**, 035404 (2006).
[29]C. Stadler, S. Hansen, A. Schöll, T.-L. Lee, J. Zegenhagen, C. Kumpf, and E. Umbach, New J. Phys. **9**, 50 (2007).
[30]I. Kröger, B. Stadtmüller, C. Kleimann, P. Rajput, and C. Kumpf, Phys. Rev. B **83**, 195414 (2011).
[31]C. González, J. Ortega, F. Flores, D. Martínez-Martin, and J. Gómez-Herrero, Phys. Rev. Lett. **102**, 106801 (2009).
[32]J. Brede, N. Atodiresei, S. Kuck, P. Lazić, V. Caciuc, Y. Morikawa, G. Hoffmann, S. Blügel, and R. Wiesendanger, Phys. Rev. Lett. **105**, 047204 (2010).
[33]Xi Chen and M. Alouani, Phys. Rev. B **82**, 094443 (2010).
[34]C. Busse, P. Lazić, R. Djemour, J. Coraux, T. Gerber, N. Atodiresei, V. Caciuc, R. Brako, A. T. N'Diaye, S. Blügel, J. Zegenhagen, and T. Michely, Phys. Rev. Lett. **107**, 036101 (2011).
[35]V. G. Ruiz, W. Liu, E. Zojer, M. Scheffler, and A. Tkatchenko, Phys. Rev. Lett. **108**, 146103 (2012).
[36]D. Vanderbilt, Phys. Rev. B **41**, 7892 (1990).
[37]P. Giannozzi *et al.*, J. Phys.: Condens. Matter **21**, 395502 (2009).
[38]J. P. Perdew, K. Burke, and M. Ernzerhof, Phys. Rev. Lett. **77**, 3865 (1996).
[39]S. Grimme, J. Comput. Chem. **27**, 1787 (2006).
[40]V. Barone, M. Casarin, D. Forrer, M. Pavone, M. Sambi, and A. Vittadini, J. Comput. Chem. **30**, 934 (2009).
[41]G. Kresse and J. Furthmüller, Comput. Mater. Sci. **6**, 15 (1996).
[42]G. Kresse and D. Joubert, Phys. Rev. B **59**, 1758 (1999).
[43]P. E. Blöchl, Phys. Rev. B **50**, 17953 (1994).
[44]T. Bučko, J. Hafner, S. Lebègue, and J. G. Ángyán, J. Phys. Chem. A **114**, 11814 (2010).
[45]P. O. Löwdin, J. Chem. Phys. **18**, 365 (1950).
[46]R. Bader, *Atoms in Molecules: A Quantum Theory* (Oxford University Press, New York, 1990).
[47]S. Tougaard, J. Electron. Spectrosc. Relat. Phenom. **178-179**, 128 (2010).
[48]I. Biswas, H. Peisert, M. Nagel, M. B. Casu, S. Schuppler, P. Nagel, E. Pellegrin, and T. Chassé, J. Chem. Phys. **126**, 174704 (2007).
[49]M. Häming, C. Scheuermann, A. Schöll, F. Reinert, and E. Umbach, J. Electron. Spectrosc. Relat. Phenom. **174**, 59 (2009).
[50]F. Evangelista, V. Carravetta, G. Stefani, B. Jansik, M. Alagia, S. Stranges, and A. Ruocco, J. Chem. Phys. **126**, 124709 (2007).
[51]E. Annese, J. Fujii, I. Vobornik, and G. Rossi, J. Phys. Chem. C **115**, 17409 (2011).
[52]The physisorption, which is also called physical adsorption, is a process in which the electronic structure of the molecule is barely perturbed upon adsorption. As a result the electronic structure of a physisorbed system can be treated using a first order perturbation theory. If not then the molecule is said to be chemisorbed.
[53]We note that further improvement including the Hubbard interaction $U = 4$ eV and exchange interaction $J = 1$ eV to better describe the $3d$ states of Mn does not significantly change the geometry of the molecule and its equilibrium distance from the substrate.
[54]R. Cuadrado, J. I. Cerdá, Y. Wang, G. Xin, R. Berndt, and H. Tang, J. Chem. Phys. **133**, 154701 (2010).
[55]H. Karacuban, M. Lange, J. Schaffert, O. Weingart, Th. Wagner, and R. Möller, Surf. Sci. **603**, L39 (2009).
[56]K. Seufert, M.-L. Bocquet, W. Auwärter, A. Weber-Bargioni, J. Reichert, N. Lorente, and J. V. Barth, Nat. Chem. **3**, 114 (2011).
[57]A. Alkauskas, A. Baratoff, and C. Bruder, Phys. Rev. B **73**, 165408 (2006).
[58]F. Djeghloul, F. Ibrahim, M. Cantoni, M. Bowen, L. Joly, S. Boukari, P. Ohresser, F. Bertran, P. Le Fèvre, P. Thakur, F. Scheurer, T. Miyamachi, R. Mattana, P. Seneor, A. Jaafar, C. Rinaldi, S. Javaid, J. Arabski, J. P. Kappler, W. Wulfhekel, N. B. Brookes, R. Bertacco, A. Taleb-Ibrahimi, M. Alouani, E. Beaurepaire, and W. Weber, Sci. Rep. **3**, 1272 (2013).
[59]P. S. Bagus, V. Staemmler, and C. Woll, Phys. Rev. Lett. **89**, 096104 (2002).
[60]L. Romaner, D. Nabok, P. Puschnig, E. Zojer, and C. Ambrosch-Draxl, New J. Phys. **11**, 053010 (2009).
[61]A. Michaelides, P. Hu, M.-H. Lee, A. Alavi, and D. A. King, Phys. Rev. Lett. **90**, 246103 (2003).
[62]P. S. Bagus, D. Käfer, G. Witte, and C. Wöll, Phys. Rev. Lett. **100**, 126101 (2008).
[63]S. Shi, G. Schmerber, J. Arabski, J.-B. Beaufrand, D. J. Kim, S. Boukari, M. Bowen, N. T. Kemp, N. Viart, G. Rogez, E. Beaurepaire, H. Aubriet, J. Petersen, C. Becker, and D. Ruch, Appl. Phys. Lett. **95**, 043303 (2009).